ELSEVIER

Polymer 40 (1999) 3165–3169

polymer

The rigid amorphous fraction of isotactic polystyrene prepared by freeze-drying from dilute solutions

Yuqin Li, Gi Xue*

Department of Polymer Science and Engineering, Nanjing University, Nanjing 210093, People's Republic of China

Received 10 March 1998; revised 1 July 1998; accepted 13 July 1998

Abstract

The techniques of wide-angle X-ray diffraction, infra-red spectroscopy and differential scanning calorimetry were used to characterize the glass transition and crystallization behavior of freeze-dried isotactic polystyrene (iPS) derived from dilute solutions. It was found that there is a concentration boundary for the original solution: below the boundary, the freeze-dried iPS samples are poorly crystallized but the chains are in a highly ordered 3_1 helix state; above the concentration boundary, the freeze-dried iPS is in a completely disordered amorphous state.

Keywords: Isotactic polystyrene; Differential scanning calorimetry; Rigid amorphous fraction

1. Introduction

Some recent measurements have focused on the consequences of rapidly taking polymers from the dilute solution regime to a concentrated state. This was interpreted as an indication that during rapid freezing, the extent of chain interpenetration which had existed in the solution would be preserved. It was possible to characterize the extent of polymer chain overlap in solutions of varying concentrations by characterizing the freeze-dried polymers. By using techniques such as fluorescence [1–3] and nuclear magnetic resonance spectroscopy (n.m.r.) [4,5], different results were obtained. Solutions containing a mixture of a polystyrene (PS) labeled with donor and acceptor fluorophores were rapidly frozen by immersing the rotating flask in liquid nitrogen, followed by vacuum sublimation of the solvent at 268 to 273 K. The resulting freeze-dried powder was pressed into a pellet, and its reflectance fluorescence was recorded. The emission spectra showed a strong increase of nonradiative energy transfer with an increase in concentration of the solution from which the sample was prepared. In particular, it was concluded that, in PS freeze-dried from a solution which was four times more dilute than the critical overlap concentration, C^*, very little chain entanglement existed. However, a solid-state ^{13}C-n.m.r dipolar dephasing experiment for a freeze-dried sample consisting of a mixture of hydrogenated and deuterated PS indicated that in such freeze-dried samples highly interpenetrated chains exist. Some infra-red (i.r.) and wide-angle X-ray diffraction (WAXD) studies indicated that the concentration boundary for chain overlap exists in the dilute region [6]. Because of these inconsistencies, further experimentation is desirable.

In this paper, differential scanning calorimetry (d.s.c.) was used to characterize freeze-dried isotactic polystyrene (iPS). It was found that the thermal behavior of a freeze-dried amorphous iPS sample depends strongly on the concentration of the original solution. Moreover, for both the amorphous iPS samples freeze-dried from dilute solutions close to the concentration boundary, the difference in thermal behavior reveals the existence of a third phase between the crystalline and the mobile amorphous phase, a metastable amorphous phase.

2. Experimental

The iPS was kindly supplied by Professor Lin Shang-An's research group at the Institute of Polymer Science, Zhong Shan University, China. ^{13}C-n.m.r. spectra showed that the iPS sample contained more than 99% isotactic triads. The number-average molecular weight of this highly stereoregular iPS was about 18×10^4. The solvent benzene was distilled before use. iPS was dissolved in the purified

---

* Corresponding author. E-mail: xuegi@nju.edu.cn

0032-3861/99/$ - see front matter © 1999 Elsevier Science Ltd. All rights reserved.
PII: S0032-3861(98)00547-3

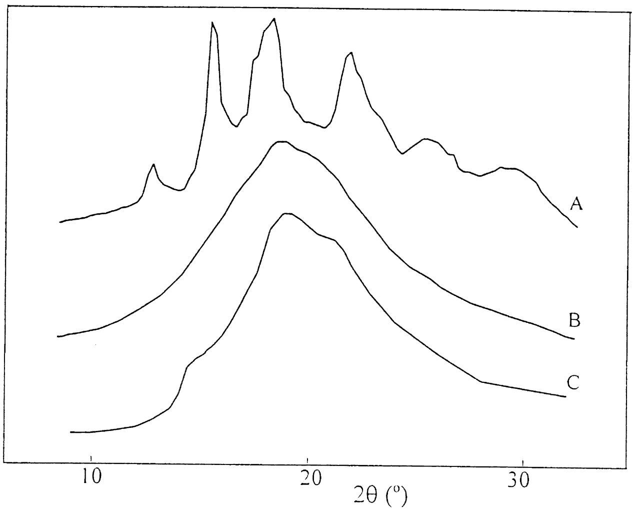

Fig. 1. Wide-angle X-ray diffraction curves recorded from: (A) freeze-dried iPS-0.07; (B) freeze-dried iPS-0.1; and (C) a highly crystallized iPS sample (iPS-0.07 after it had been heated to 460 K at 20 K min^{-1} in the d.s.c. pan).

benzene to make very dilute solutions with concentrations of 0.04, 0.07, 0.1 and 0.3 wt% at 343 K. The warm solution was injected directly into liquid nitrogen so that it was frozen in a fraction of a second. The frozen solvent was then sublimed in vacuum at 268 to 273 K. The resulting iPS powders were designated as samples iPS-0.04, iPS-0.07, iPS-0.1 and iPS-0.3, respectively. They were examined by d.s.c. (Perkin–Elmer model DSC-2C system with a data station), i.r. (IFS 66V vacuum-type FT-IR spectrophotometer), and wide-angle X-ray diffraction (Rigaku D/Max-Ra diffractometer).

3. Results and discussion

In Fig. 1(A) and Fig. 1(B) are shown the WAXD patterns of iPS-0.07 and iPS-0.1, respectively. For comparison, a WAXD pattern recorded from a highly crystallized iPS is shown in Fig. 1(C). Fig. 1(B) exhibits a broad and intense band, with the center at $2\theta = 18.4°$. The diffraction pattern of iPS-0.3 is similar to that shown in Fig. 1(B). It is obvious that these two samples, iPS-0.1 and iPS-0.3, are mainly in the amorphous phase. Small differences can be found between Fig. 1(A) and Fig. 1(B). Two minor peaks at $2\theta = 14.3°$ and 21.7° exist in Fig. 1(A), which indicates that it is partly crystalline. The crystallinity of iPS-0.07 (Fig. 1(A)), calculated from the WAXD pattern according to the method of Challa et al. [7], is 7%. The diffraction pattern of iPS-0.04 is similar to that shown in Fig. 1(A). The crystallinity of iPS-0.04 obtained by WAXD is 9%.

A similar result concerning the crystallinity of the freeze-dried samples can be obtained from the i.r. spectra. In Fig. 2, the i.r. spectra recorded from iPS-0.04 and iPS-0.07 (Fig. 2(A) and Fig. 2(B)) are compared with those measured

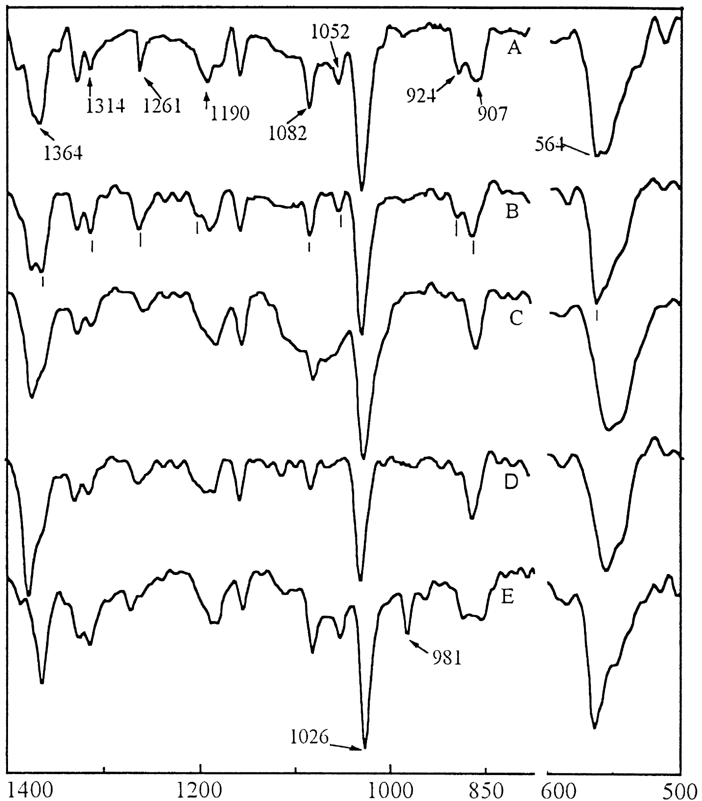

Fig. 2. I.r. spectra recorded from freeze-dried samples: (A) iPS-0.04; (B) iPS-0.07; (C) iPS-0.1; (D) iPS-0.3; and (E) a highly crystallized iPS sample.

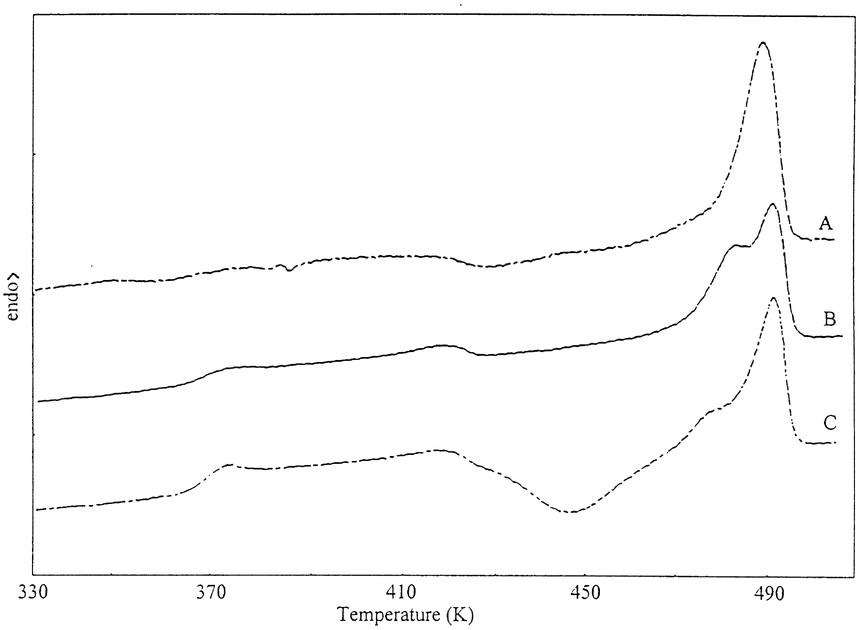

Fig. 3. D.s.c. curves of freeze-dried iPS-0.07: (A) the first scan from 310 to 510 K; (B) the second scan; and (C) the third scan.

from iPS-0.1 and iPS-0.3 (Fig. 2(C) and Fig. 2(D)). For comparison, a spectrum of highly crystallized iPS is shown in Fig. 2(E). The 981 cm^{-1} band, shown in Fig. 2(E), behaves as a typical crystallization-sensitive band with the intensity proportional to the degree of crystallinity [8]. This crystallization-sensitive band remains at a low level for iPS-0.04 and iPS-0.07 (Fig. 2(A) and Fig. 2(B)). The crystallinity of these two samples can be calculated from the known crystallinity of the highly crystalline sample (Fig. 2(E)) and the relative intensity of $I_{981\ cm^{-1}}/I_{1026\ cm^{-1}}$ [9]; they are 8% and 7%, respectively. However, in the spectra of samples iPS-0.04 and iPS-0.07, the isotactic $(TG)_3$ helix absorption bands at 1364, 1314, 1261, 1190, 1082, 1052, 924, 907 and 564 cm^{-1} (indicated by short lines in Fig. 2(A) and Fig. 2(B)), which are associated with intramolecular interactions within one molecular chain [8,10], show intensities as strong as those in a highly crystallized sample (Fig. 2(E)). The i.r. spectra confirmed the result obtained from the WAXD pattern that iPS-0.04 and iPS-0.07 are poorly crystallized, their crystallinity being no more than 10%. Moreover, the i.r. spectra also indicated that the iPS chains in the very dilute solution ($C \leq 0.07$ wt%) as well as those in the freeze-dried state are in a highly ordered 3_1 helix state. As these very dilute solutions were frozen rapidly, some helical segments aggregated into crystal nuclei, resulting in a freeze-dried iPS with some crystals formed in a fraction of a second. In the spectra of other two samples (iPS-0.1 and iPS-0.3), the absence of the bands at 1364 and 1197 cm^{-1}, the reduction in intensity of the 1314 and 1261 cm^{-1} bands, the singlet bands at 1079 and 908 cm^{-1}, and the shift from 564 cm^{-1} to 555 cm^{-1} reveal that the chains of these two iPS samples are in a disordered state [8–10].

Figs 3 and 4 show the d.s.c. thermograms of freeze-dried samples of iPS-0.07 and iPS-0.1, respectively. The d.s.c. curves of iPS-0.04, which were similar to Fig. 3 (iPS-0.07), and those of iPS-0.3, which were similar to Fig. 4 (iPS-0.1), are omitted. They were first scanned from 310 to 510 K (curves A), followed by cooling to 310 K at 5 K min^{-1}. A second scan from 310 to 510 K was then carried out (curves B) followed by cooling to 310 K at 320 K min^{-1}. Then the third scan from 310 to 510 K was taken (curves C). All of the heating rates were 20 K min^{-1}.

The d.s.c. heating curve for ordinary semicrystalline iPS usually shows a glass transition in the region of 363–373 K. It is generally considered that the change of heat capacity at the glass transition temperature (T_g) reveals the content of the amorphous part of the sample. For samples iPS-0.04 and iPS-0.07, their first-run scans show no measurable or very little glass transition (Fig. 3(A)). Their change in heat capacity (ΔC_p) at T_g is 0 and 1.05×10^{-2} cal g^{-1} K^{-1}, respectively. It can be calculated from ΔC_p that the amorphous fraction (f_{MAM}) in these two samples is 0% and 13%, respectively. These conclusions are inconsistent with the WAXD pattern and the i.r. spectra, which indicated that iPS-0.04 and iPS-0.07 are mainly in the amorphous state as shown in Figs 1 and 2. Generally, what we get from the X-ray diffraction pattern is the situation about the three-dimensional order of samples. Most of that three-dimensional disordered part in iPS-0.04 and iPS-0.07 reflected by the X-ray diffraction does not show the change of heat capacity around T_g. I.r. spectra (Fig. 2(A) and Fig. 2(B)) confirmed that the three-dimensional disordered fraction of iPS-0.04 and iPS-0.07 has highly ordered 3_1 helix chains although they are not in the crystalline state. It is presumed that it is these highly ordered chains that

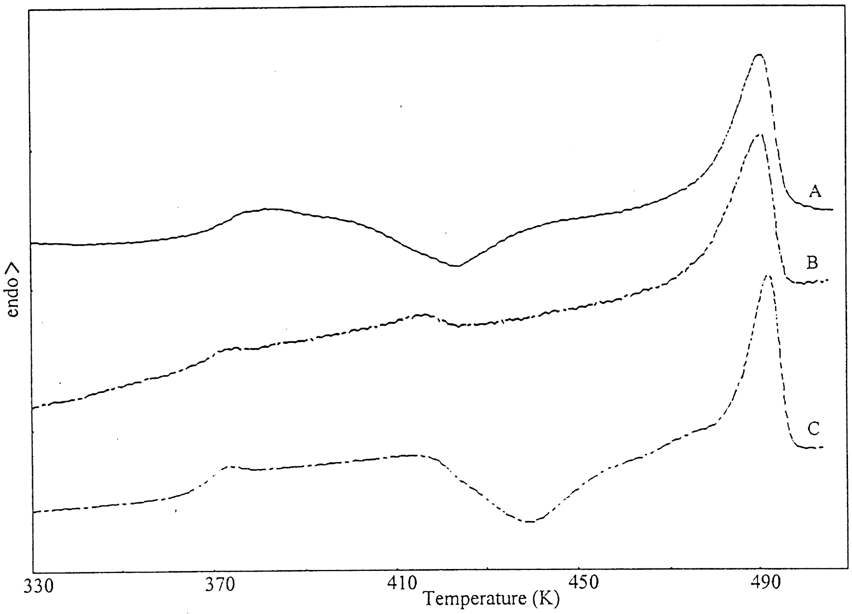

Fig. 4. D.s.c. curves of freeze-dried iPS-0.1: (A) the first scan from 310 to 510 K; (B) the second scan; and (C) the third scan.

show no glass transition. For a normal amorphous sample, only the smaller units such as pendant groups and branched groups can move, but the conformation cannot be changed below T_g. Upon heating to T_g, the movement of chain segments is activated, and conformational transitions can be realized. The change of heat capacity at the glass transition temperature reflects the difference in mobility of the chains. If the iPS chains are highly ordered with a 3_1 helix conformation, their total energy is lower and they require higher energy to change conformation. The local motion is then restricted by the helix structure and the chains cannot move just above T_g. It is this amorphous part with highly ordered chains that has no glass transition. A contradiction resulted from the wrong attribution of this special amorphous phase. Since it has no glass transition, it was considered as the crystalline part in the d.s.c. thermogram, and since it does not show crystal diffraction, it was considered as the amorphous part in the WAXD pattern. It is actually an intermediate state between the crystalline and the usual amorphous phase. This intermediate state is highly ordered in the chain but it is three-dimensional disordered. This third phase was called the rigid amorphous fraction (RAF) or the metastable state in several polymers such as polypropylene [11], poly(oxymethylene) [12] and in polymers with less flexible structures such as poly(phenylene sulfide) [13]. To our knowledge, no papers have ever dealt with the RAF of iPS.

The WAXD pattern in Fig. 1(C), which was described as a highly crystalline iPS, was recorded from iPS-0.07 after it had been heated to 460 K (before the onset of melting) in the d.s.c. pan at 20 K min^{-1}. It exhibits several sharp peaks in the $2\theta = 10$–$30°$ range of the diffractogram, indicating that the sample is highly crystallized. Its crystallinity calculated from its WAXD pattern is 55%. During heating from 310 to 460 K at a rate of 20 K min^{-1}, the crystallinity (obtained from the WAXD pattern) of the sample increases drastically (from 7% to 55%) but the crystalline exothermic value in this d.s.c. curve as shown in Fig. 3(A) is very small (-0.47 cal g^{-1}) compared with the melting endothermic peak (5.88 cal g^{-1}), indicating that little heat is required to induce crystallization of the RAF of iPS-0.07. This confirms that the state of the chains in this special amorphous phase is close to the crystalline state. This result is in accordance with the conclusion that most of the chains are in the highly ordered helix state with lower energy [14]. The curve changes its shape somewhat for the second scan of iPS-0.07 as shown in Fig. 3(B). The third scan shown in Fig. 3(C) is the same as the d.s.c. curve of a normal amorphous iPS: the glass transition is prominent and the heat capacity of the crystalline exothermic peak becomes large. The complete difference between the first scan (Fig. 3(A)) and the third scan (Fig. 3(C)) illustrates the difference between the amorphous phase in the original iPS-0.04 and iPS-0.07 (freeze-dried from the dilute solution $C \leq 0.07$ wt%) and ordinary amorphous iPS (frozen from the melt). Moreover, the original freeze-dried iPS-0.04 and iPS-0.07 turn back into the ordinary state after being repeatedly heated and cooled. However, for the other two samples iPS-0.1 and iPS-0.3, the first scan (Fig. 4(A)) exhibits a glass transition at 363–368 K. When iPS-0.1 and iPS-0.3 are freeze-dried from their parent solutions, they are in a nonequilibrium state. During heating to near T_g, some groups of the chains begin to move and turn slowly to the equilibrium state. So they show no hysteresis capacity. There is also a large crystalline exothermic peak which is comparable to the melting endothermic peak in the same d.s.c. curve, and which is similar to a typical amorphous iPS sample. The similarity of the first-run scan (Fig. 4(A)) and the third-run scan (Fig. 4(C)) of iPS-0.1 and iPS-0.3 indicates that the samples freeze-dried from less dilute solutions (concentration $C \geq 0.1$ wt%) are in a similar state as those frozen from the melt, although the crystallization temperature of the former is somewhat lower than that of the latter. This is ascribed to the nonequilibrium state or the isolated state of the chains of the former [1,2]. All of these observations suggest that iPS-0.1 and iPS-0.3 are in the ordinary amorphous state, i.e., the mobile amorphous state.

Quantitative data about the RAF in freeze-dried iPS-0.04, iPS-0.07, iPS-0.1 and iPS-0.3 samples can be obtained from the equation of Grebowicz et al. [11]. They considered that, under appropriate assumptions, the magnitude (or the strength) of the glass transition in a semicrystalline polymer is proportional to the amount of free (or mobile) amorphous phase in the semicrystalline polymer, and another variable — termed the rigid amorphous fraction — represents the amorphous phase that does not contribute to the strength of the glass transition. They defined a variable f_{RAF} as:

$$f_{\mathrm{RAF}} = 1 - \frac{\Delta C_{\mathrm{p}}^{\mathrm{sc}}}{\Delta C_{\mathrm{p}}^{\mathrm{am}}} - C_{\mathrm{r}}$$

where ΔC_{p} is the change in heat capacity at T_{g}. The superscripts sc and am refer to the semicrystalline and amorphous materials, respectively. C_{r} is the crystallinity of the sample. Using this equation, the f_{RAF}s were obtained and are listed in Table 1. The following points are noteworthy. (1) When iPS powders are freeze-dried from their parent solutions, they are fine particles and their surface area is extremely large; thus their endothermic values deviate highly from that of a normal semicrystalline sample. Moreover, the samples crystallize during heating. The endothermic values do not reflect their original state. So the variable C_{r} is calculated from the WAXD patterns. (2) The samples for the third-run scans of the d.s.c. are all considered as being in the amorphous state and their crystallinity is 0%, since they were obtained by cooling the melt at a rate of 320 K min^{-1}. Table 1 shows that two kinds of amorphous phase are obtained when iPS samples are freeze-dried from dilute solutions: the normal amorphous fraction and the rigid amorphous fraction. The acquisition of the RAF depends strongly on the original concentration. When $C \geq 0.1$ wt%, the freeze-dried iPS samples are fully in the mobile amorphous state within the range of experimental error. However, when $C \leq 0.07$ wt%, the freeze-dried samples have a large (as much as 80% and above) rigid amorphous fraction. This concentration boundary coincides with that from the i.r. spectra and WAXD pattern. Table 1 also shows that the RAF of the iPS would turn into the mobile amorphous phase gradually after repeated melting and cooling.

Table 1
The rigid amorphous fraction in four freeze-dried iPS samples obtained from d.s.c. thermograms

		f_{MAM}	C_{r}	f_{RAF}
iPS-0.04	First scan	0	9	91
	Second scan	0	—	—
	Third scan	73	0	27
iPS-0.07	First scan	13	7	80
	Second scan	45	—	—
	Third scan	91	0	9
iPS-0.1	First scan	97	0	3
	Second scan	70	—	—
	Third scan	101	0	−1
iPS-0.3	First scan	97	0	3
	Second scan	71	—	—
	Third scan	100	0	0

The mobile amorphous fraction, $f_{\mathrm{MAM}} = \Delta C_{\mathrm{p}}^{\mathrm{sc}}/\Delta C_{\mathrm{p}}^{\mathrm{am}}$.
The rigid amorphous fraction, $f_{\mathrm{RAF}} = 1 - f_{\mathrm{MAM}} - C_{\mathrm{r}}$.
$\Delta C_{\mathrm{p}}^{\mathrm{am}}$ for PS is 7.90×10^{-2} cal g^{-1} K^{-1} [15].

Acknowledgements

We are grateful for the support from the National Science Foundation of China and the State Key Laboratory of Polymeric Materials of Sichuan Union University.

References

[1] Morawetz H. Science 1988;240:172.
[2] Chang LP, Morawetz H. Macromolecules 1987;20:428.
[3] Doi M, Edwards SF. The theory of polymer dynamics. Oxford, UK: Clarendon Press, 1986.
[4] McGrath KJ, Roland CM. Macromolecules 1992;25:1366.
[5] McGrath KJ, Roland CM, Weiss RG. Macromolecules 1993;26:6127.
[6] Xue G, Wang Y, Gu X, Lu Y. Macromolecules 1995;28:4344.
[7] Challa G, Hermans PH, Weidinger A. Makromol Chem 1969;55:169.
[8] Nakoaki T, Kobayashi M. J Mol Struct 1991;242:315.
[9] Painter PC, Koenig JL. J Polym Sci, Polym Phys Edn 1975;13:1809.
[10] Kobayashi M, Nakaoki T. Macromolecules 1990;23:78.
[11] Grebowicz J, Law SF, Wunderlich B. J Polym Sci, Polym Symp 1984;71:19.
[12] Suzuki H, Grebowicz J, Wunderlich B. Makromol Chem 1985;186:1109.
[13] Cheng SZD, Wu Z, Wunderlich B. Macromolecules 1987;20:2802.
[14] Itagaki H, Takahashi I. Macromolecules 1995;28:5477.
[15] Wunderlich B, Jones LD. J Macromol Sci — Phys 1969;B3:67.